Pulsed-Laser Transient Testing with Tunable Wavelength and High Resolution for High Mobility MOSFETs

Kai Ni, *Student Member, IEEE*, Andrew L. Sternberg, *Member, IEEE*, En Xia Zhang, *Senior Member, IEEE*, John A. Kozub, Rong Jiang, *Student Member, IEEE*, Ronald D. Schrimpf, *Fellow, IEEE*, Robert A. Reed, *Fellow, IEEE*, Daniel M. Fleetwood, *Fellow, IEEE*, Michael L. Alles, *Member, IEEE*, Jianqiang Lin, *Student Member, IEEE*, Alon Vardi, *Student Member, IEEE*, Jesus del Alamo, *Fellow, IEEE*

***Abstract*—A tunable wavelength laser system and high resolution transient capture system are introduced to characterize transients in high mobility MOSFETs. The new setup enables resolution of fast transient signals and understanding of charge collection mechanisms.**

***Index Terms*—GaAs, InGaAs, III-V, MOSFETs, single-event transient, charge collection, two-photon- absorption (TPA)**

I. Introduction

Pulsed-laser testing has become a valuable testing method to study single event effects (SEE) in devices and circuits [1], [2]. Although the charge generation mechanisms and charge profile induced by laser irradiation are different from heavy ion irradiation, laser testing provides a complementary nondestructive, convenient, and low-cost method to identify mechanisms responsible for SEE. Pulsed laser testing is generally divided into two categories: single-photon absorption (SPA) and two-photon absorption (TPA), depending on the electron-hole pair generation mechanism [3].

SPA refers to above-bandgap optical excitation, where each absorbed photon generates an electron-hole pair. Due to the exponential decay of light intensity traveling through the material, the penetration depth of the laser is limited. To generate charge tracks with various depths, usually the laser wavelength is varied [4]. For SPA irradiation, however, it is often difficult or impossible to inject charge into a device, due to the presence of metal over-layers. This challenge is addressed by TPA, which is produced by irradiation with high peak power femtosecond laser pulses at subbandgap wavelength. Electron-hole pairs are only generated in the focal region of the laser beam, where the optical field intensity is high enough to stimulate the absorption of two photons simultaneously. This enables backside irradiation, thus addressing the problem of metal over-layers.

This work was supported by the Defense Threat Reduction Agency through its fundamental research program.

K. Ni, A. L. Sternberg, E. X. Zhang, R. Jiang, R. D. Schrimpf, R. A. Reed, D. M. Fleetwood, and M. L. Alles are with the Department of Electrical Engineering and Computer Science, Vanderbilt University, Nashville, TN 37235 USA (e-mail: kai.ni@vanderbilt.edu).

J. A. Kozub is with the Department of Physics, Vanderbilt University, Nashville, TN USA.

J. Lin, A. Vardi, and J. A. del Alamo are with Microsystems Technology Laboratories, Massachusetts Institute of Technology, Cambridge, MA 02139, USA.

Typically, the TPA laser wavelength is set to be around 1260 nm, at which the photon energy is slightly smaller than the Si bandgap. However, with CMOS scaling continuing to sub-10 nm nodes, high mobility channel materials, such as InGaAs/Ge, are likely to be introduced [5], [6]. The integration of these new materials will also necessitate other relevant materials, creating a multi-layer structure. There are multiple bandgaps in these advanced devices compared with Si. Therefore, a single laser wavelength tuned for Si is not optimal for these new materials. Charge generation at a wavelength of 1260 nm will lead to mixed SPA and TPA in different layers, depending on material bandgaps, such as shown in [7], [8], [9]. In studying the charge collection mechanisms in these multi-layer structure devices, it is both necessary and difficult to identify the roles of different layers. Thus a laser with tunable wavelength is helpful to inject charge into a specific layer only, e.g., the channel layer.

Time-resolved measurements are usually conducted with digital sampling oscilloscopes. For fast transients or fast edges characterization, it is desirable to have enough time resolution to resolve ultrafast signals. The highest bandwidth oscilloscope reported is a 70 GHz superconducting sampling oscilloscope, which has sub-10 ps resolution [10]. However, this oscilloscope needs additional cooling and can only capture limited time window transients, so it is not practical for most testing. Almost all the other transient capture experiments that have been reported are conducted with oscilloscopes with bandwidths less than or approximately equal to 20 GHz [7], [8], [9], [11]. These have limited capability to resolve fast transient signals.

In this paper, we describe a tunable wavelength laser system that can inject charge into a specific layer in the device and capture transients with a 36 GHz bandwidth oscilloscope. We show that these new capabilities lead to enhanced insight into charge collection mechanisms in advanced devices.

II. Device Descriptions

Two types of devices are tested, as shown in Fig. 1 (a) and (b), respectively. The first is a planar InGaAs quantum-well MOSFET. The detailed fabrication process is described in [12]. A 0.4 μm thick $In_{0.52}Al_{0.48}As$ buffer layer is grown on a 600 μm thick semi-insulating InP substrate. A 5 nm thick $In_{0.7}Ga_{0.3}As$ channel is grown on top of the buffer layer. A silicon delta doping layer (*n*-type) in the buffer just below the channel is used to enhance the channel electron density. 2.5 nm of HfO_2 as gate dielectric is deposited by atomic layer deposition directly on top of the channel. The planar device was tested to compare the old limited bandwidth transient capture system

with the new higher bandwidth system. The tested device has a gate length of 100 nm and gate width of 10 μm.

The other type of device is a double-gate InGaAs FinFET. The detailed fabrication process is presented in [13]. A 40 nm thick $In_{0.53}Ga_{0.47}As$ channel is grown on top of a 0.4 μm $In_{0.52}Al_{0.48}As$ buffer. The fin width and height are 20 nm and 220 nm, respectively. The tested device has a gate length of 50 nm. The FinFET device was tested with a pulsed-laser at different wavelengths. For transient capture, all the devices are mounted in custom-milled metal packages with microstrip transmission lines and Precision 2.92 mm K connectors [7], [8].

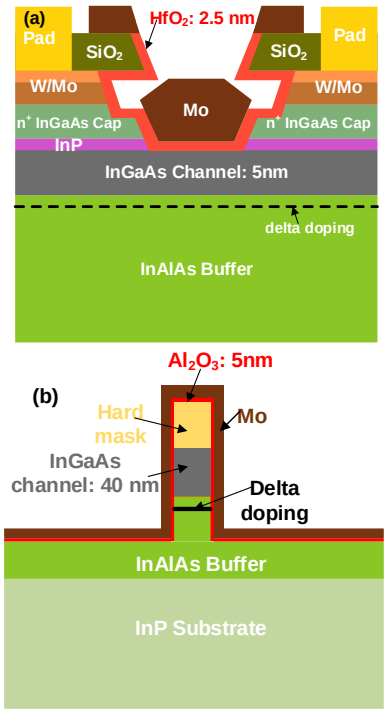

Fig. 1. Schematic diagram of (a) planar InGaAs quantum-well MOSFET and (b) InGaAs FinFET.

III. Experimental Setup

Pulsed-laser testing experiments were performed at Vanderbilt University. The laser system setup is shown schematically in Fig. 2 [14]. It utilizes a titanium-sapphire (Ti/S) pumped Optical Parametric Generator (OPG). The OPG is pumped at 1 kHz repetition rate with 1 mJ, 150 fs pulses centered at 800 nm from a chirped-pulse amplifier. The amplifier is seeded with a passively mode-locked Ti/S oscillator. The OPG uses non-linear parametric frequency conversion in a Beta Barium Borate (BBO) crystal to generate and amplify signal and idler wavelengths that are continuously tunable from ~1200 nm to ~2400 nm. Using harmonic, sum, and difference frequency-generating crystals outside the OPG, wavelengths from ~200 nm to ~10 µm can be generated with average pulse energies varying from 1µJ/pulse to 100µJ/pulse, depending on the wavelength. A prism is used to isolate the desired wavelength from the output of the laser system. Optics currently installed on the beam line allow for component testing at wavelengths from 300 nm to 2600 nm.

The selected wavelength is spatially filtered and variably attenuated using holographic wire-grid polarizers before reaching the test bench. The laser beam passes through a series of beam splitters before reaching the target. The first beam splitter diverts a fraction of the beam to a calibrated photodetector. Each pulse from the detector is captured and measured individually. Another beam splitter couples a broadband near-IR light source onto the beam axis for illuminating the target, and a third sends light reflected from the target to an IR camera for imaging and positioning of the laser spot. Finally, the laser is focused through the back-side of the target using either a 50X or 100X microscope objective mounted to a customized high-precision z-stage used to change the depth at which the laser focuses inside the die.

The laser wavelengths used in this experiment are 1260 nm and 2200 nm. The photon energy and carrier generation mechanism are listed in Table I for different materials in the device. For a wavelength of 1260 nm, charge will be generated in all the semiconductor materials, either through SPA or TPA. In contrast, for a wavelength of 2200 nm, charge can only be generated in the $In_{0.53}Ga_{0.47}As$ channel. No charge will be generated in the $In_{0.52}Al_{0.48}As$ or InP, since the photon energy is less than half of the material bandgap so that neither SPA nor TPA can take place. Therefore, charge can be generated in a specific layer, allowing the response of that specific layer to be isolated from all the surrounding layers.

The transients were captured using a Tektronix TDS6124C oscilloscope with 12 GHz front-end bandwidth and 20 GS/s sampling rate and a Teledyne Lecroy LabMaster 10-36Zi-A oscilloscope with 36 GHz front-end bandwidth and 80 GS/s sampling rate. During these tests, the source was grounded, the drain bias was 0.5 V, and the gate bias was varied. A semiconductor parameter analyzer, HP 4156B, supplied the dc biases through Picosecond Model 5542 bias tees with 50 GHz bandwidth.

TABLE I
MATERIALS PARAMETERS AND CARRIER GENERATION MECHANISM AT TWO DIFFERENT WAVELENGTH

Material	Bandgap	λ=1260 nm (E=0.98 eV)	λ=2200 nm (E=0.56 eV)
$In_{0.53}Ga_{0.47}As$	0.75 eV	**SPA**/TPA	TPA
$In_{0.52}Al_{0.48}As$	1.46 eV	TPA	NONE
InP	1.35 eV	TPA	NONE

(For materials where both SPA and TPA happen, the dominant mechanism is marked as bold.)

IV. Results and Discussions

Charge collection mechanisms in planar InGaAs quantum-well MOSFET have been discussed in [7]. Here we compare the transients captured by the two different oscilloscopes irradiated by a 1260 nm laser. Fig. 3 (a) and (b) show the transients captured by the TDS6124C and LabMaster 10-36Zi-A oscilloscopes, respectively. The rise time of the transients is very short, on the order of 100 ps. As a result, only a single data point is recorded on the rising edge for the TDS6124C oscilloscope, which has 50 ps resolution. It is hard to predict the rising edge shape based on such limited data points. However, for the LabMaster 10-36Zi-A oscilloscope, the time resolution is 12.5 ps, which is short enough to resolve the rising edge. By fitting the rising edge with an exponential, the rise time constant is estimated to be around 39 ps. This illustrates both the benefit

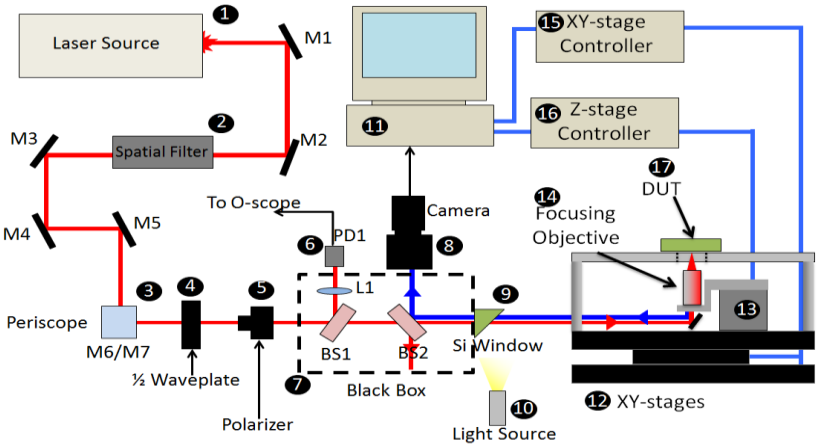

Fig. 2. A simplified block diagram of TPA test setup (after [14]).

and the need to use a higher bandwidth system to characterize fast signals with more accuracy and precision

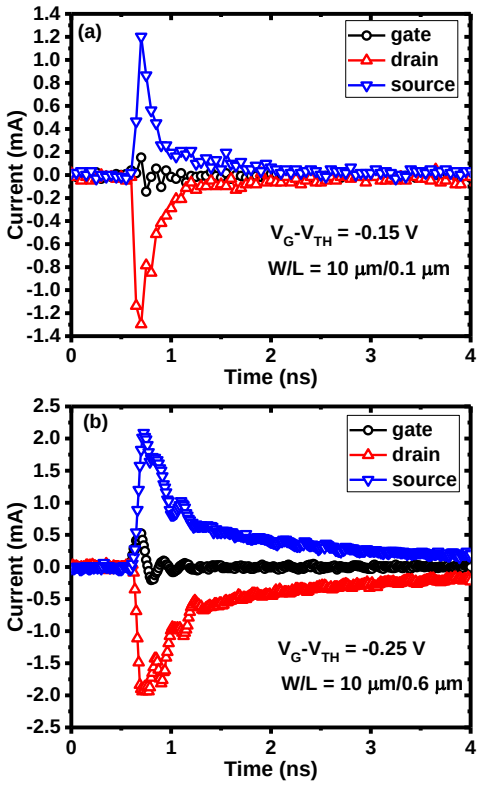

Fig. 3. Typical transients captured by (a) Tektronix TDS6124C oscilloscope and (b) Teledyne Lecroy LabMaster 10-36Zi-A oscilloscope. The strike point locates at the center of the device, on top of the gate. The laser wavelength used is 1260 nm. Peak currents differ as a result of different laser energies.

Another feature of the transients shown in Fig. 3(b) is the oscillation signal appearing in the transients. The period of oscillation is 0.2 ns. There are many possible reasons for this oscillation, including impedance mismatch and extrinsic RLC oscillation associated with bond wires [15]. Since the bond wire used for this device is relatively long, a few mm, here it is likely related to RLC oscillation [15].

Charge collection in InGaAs FinFET devices is compared with two different wavelengths, 1260 nm and 2200 nm, in Fig. 4(a) and (b). Two typical transients are shown, for a device biased in the ON state. The rising edge is well resolved and the relevant time constant is about 40 ps, similar to the planar device. The oscillation is still present in the gate transients, with a period of 0.15 ns. This likely results from the shorter bond wires used in the FinFET, as compared with the planar device. One big difference between the two wavelengths is the transient shape. The transient fall times are faster at a wavelength of 2200 nm than at 1260 nm. The time constants obtained by fitting the transients with double exponentials at 2200 nm, 0.14 ns and 0.66 ns, are less than half of those at 1260 nm, 0.28 ns and 1.50 ns. This is probably because charges are only generated in the channel at 2200 nm, so they can quickly get collected.

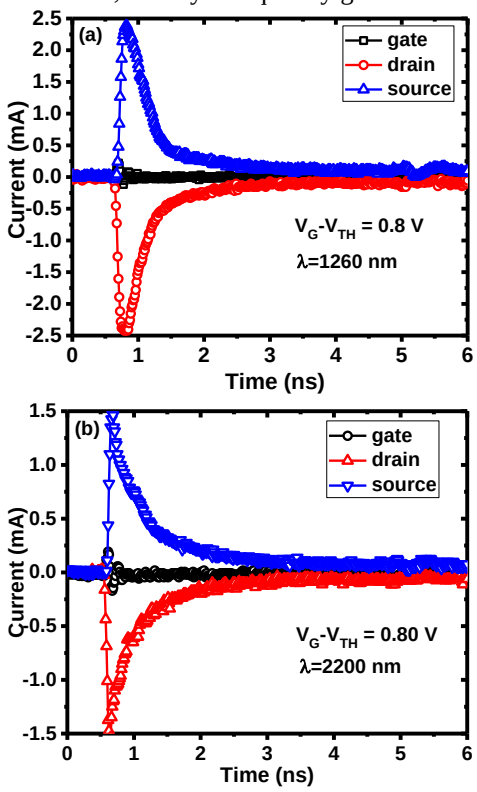

Fig. 4. Typical transients captured by Teledyne Lecroy LabMaster 10-36Zi-A oscilloscope at (a) λ=1260 nm and (b) λ=2200 nm at V_G-V_{TH}=0.8 V.

Another mechanism that the tunable wavelength laser can illustrate clearly is the observed long transient tail when a device is biased in the ON state [16]. It is ascribed to the carrier trapping and subsequent thermal release in the deep traps in the buffer and substrate. The tail usually lasts on the order of µs or ms, corresponding to the trap time constant. If charges are only

generated in the channel, then the effect of buffer and substrate can be minimized.

Fig. 5 (a) and (b) show the same drain transients as Fig. 4 (a) and (b), but with a time window of 200 ns at wavelengths of 1260 nm and 2200 nm. In both cases, long tails are observed, although the magnitudes are small. The smaller magnitude for the FinFET compared with the planar transistor [16] is due to its small fin width, which leads to reduced effects of the buffer and substrate layers on the active region. The long tails observed for both wavelengths suggests that the deep traps in the buffer and substrate are not the only sources that cause the long tails. They do make a contribution, however, since the tail current at 2200 nm, 16 μA, is approximately one half that at 1260 nm, 33 μA. Therefore, tunable wavelength laser irradiation provides a method to distinguish the channel response from that of other layers.

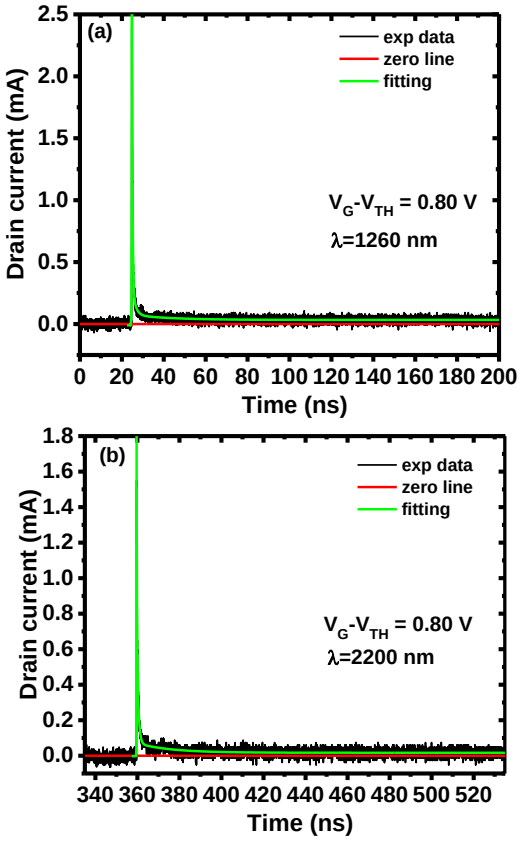

Fig. 5. Typical drain transients captured by Teledyne Lecroy LabMaster 10-36Zi-A oscilloscope at (a) λ=1260 nm and (b) λ=2200 nm at V_G-V_{TH}=0.8 V. The time window is 200 ns.

V. Conclusions

In this paper, a tunable wavelength laser system and high resolution transient capture system are introduced for high mobility MOSFETs. With high time resolution, transient features, such as fast edges and oscillations, are well resolved. The tunable wavelength laser provides a method to generate charge only in a specific layer, usually the channel layer, since the lowest bandgap typically occurs in the channel of high mobility MOSFETs. This enables the response of the channel layer to be distinguished from that of the surrounding layers, providing a valuable tool to understand charge collection mechanisms in advanced devices.

References

[1] J. S. Melinger, S. Buchner, D. McMorrow, W. J. Stapor, T. R. Weatherford, and A. B. Campbell, "Critical evaluation of the pulsed laser method for single event effects testing and fundamental studies," *IEEE Trans. Nucl. Sci.*, vol. 41, no. 6, pp. 2574-2584, Dec. 1994

[2] S. Buchner, F. Miller, V. Pouget, and D. McMorrow, "Pulsed-laser testing for single-event effects investigations," *IEEE Trans. Nucl. Sci.*, vol. 60, no. 3, pp. 1852-1875, Jun. 2013

[3] D. McMorrow, W. T. Lotshaw, J. S. Melinger, S. Buchner, and R. L. Pease, "Subbandgap laser-induced single event effects: carrier generation via two-photon absorption," *IEEE Trans. Nucl. Sci.,* vol. 49, no. 6, pp. 3002-3008, Dec. 2002

[4] J. S. Melinger, D. McMorrow, A. B. Campbell, S. Buchner, L. H. Tran, A. R. Knudson, and W. R. Curtice, "Pulsed laser-induced single event upset and charge collection measurements as a function of optical penetration depth," *J. Appl. Phys.*, vol. 84, no. 2, pp. 690-703, Jul. 1998

[5] J. A. del Alamo, "Nanometre-scale electronics with III-V compound semiconductors," *Nature*, vol. 479, no. 7373, pp. 317-323, Nov. 2011.

[6] K. J. Kuhn, "Considerations for ultimate CMOS scaling," *IEEE Trans. Electron Devices*, vol. 59, no. 7, pp. 1813-1828, Jul. 2012

[7] K. Ni, E. X. Zhang, N. C. Hooten, W. G. Bennett, M. W. McCurdy, A. L. Sternberg, R. D. Schrimpf, R. A. Reed, D. M. Fleetwood, M. L. Alles, K. Tae-Woo, L. Jianqiang, and J. A. del Alamo, "Single-event transient response of InGaAs MOSFETs," *IEEE Trans. Nucl. Sci.,* vol. 61, no. 6, pp. 3550-3556, Dec. 2014.

[8] E. X. Zhang, I. K. Samsel, N. C. Hooten, W. G. Bennett, E. D. Funkhouser, K. Ni, D. R. Ball, M. W. McCurdy, D. M. Fleetwood, R. A. Reed, M. L. Alles, R. D. Schrimpf, D. Linten, and J. Mitard, "Heavy-ion and laser induced charge collection in SiGe channel pMOSFETs," *IEEE Trans. Nucl. Sci.,* vol. 61, no. 6, pp. 3187-3192, Dec. 2014.

[9] I. K. Samsel, E. X. Zhang, A. L. Sternberg, K. Ni, R. A. Reed, D. M. Fleetwood, M. L. Alles, R. D. Schrimpf, D. Linten, J. Mitard, L. Witters, and N. Collaert, "Charge collection mechanisms of Ge-channel bulk pMOSFETs," *IEEE Trans. Nucl. Sci.,* vol. 62, no. 6, pp. 2725-2731, Dec. 2015.

[10] R. S. Wagner, N. Bordes, J. M. Bradley, C. J. Maggiore, A. R. Knudson, and A. B. Campbell, "Alpha, boron, silicon and iron ion-induced current transients in low-capacitance silicon and GaAs diodes," *IEEE Trans. Nucl. Sci.,* vol. 35, no. 6, pp. 1578-1584, Dec. 1988.

[11] D. McMorrow, J. Warner, S. Dasgupta, V. Ramachandran, J. B. Boos, R. A. Reed, R. D. Schrimpf, P. Paillet, V. F. Cavrois, J. Baggio, S. Buchner, F. E. Mamouni, M. Raine, and O. Duhamel, "Novel energy dependent effects revealed in GeV heavy ion induced transient measurements of antimony-based III-V HEMTs," *IEEE Trans. Nucl. Sci.,* vol. 57, no. 6, pp. 3358-3365, Dec. 2010

[12] L. Jianqiang, Z. Xin, Y. Tao, D. A. Antoniadis, and J. A. del Alamo, "A new self-aligned quantum-well MOSFET architecture fabricated by a scalable tight-pitch process.", *Proc. IEEE Int. Electron Device Meeting (IEDM),* pp. 421-424, 2013

[13] A. Vardi, X. Zhao, and J. A. del Alamo, "Quantum-size effects in sub 10-nm fin width InGaAs FinFET," *IEEE Int. Electron Device Meeting (IEDM),* pp. 31.3.1-31.3.4, 2015

[14] N. C. Hooten, "Charge collection mechanisms in silicon devices during high-level carrier generation events," Ph.D. dissertation, Vanderbilt University, 2014

[15] D. McMorrow, A. R. Knudson, and A. B. Campbell, "Fast charge collection in GaAs MESFETs," *IEEE Trans. Nucl. Sci.,* vol. 37, no. 6, pp. 1902-1908, Dec. 1990.

[16] K. Ni, E. X. Zhang, I. K. Samsel, R. D. Schrimpf, R. A. Reed, D. M. Fleetwood, A. L. Sternberg, M. W. McCurdy, S. Ren, T. P. Ma, L. Dong, J. Y. Zhang, P. D. Ye, "Charge collection mechanisms in GaAs MOSFETs," *IEEE Trans. Nucl. Sci.*, vol. 62, no. 6, pp. 2752-2759, Dec. 2015